The amino acid transporter *pfaat1* modulates chloroquine resistance and fitness in malaria parasites

Alfred Amambua-Ngwa[1*], Katrina A. Button-Simons[2*], Xue Li[3*], Sudhir Kumar[4*], Katelyn Vendrely Brenneman[2*], Marco Ferrari[3], Lisa A. Checkley[2], Meseret T. Haile[4], Douglas A. Shoue[2], Marina McDew-White[3], Sarah M. Tindall[5], Ann Reyes[3], Elizabeth Delgado[3], Haley Dalhoff [2], James K. Larbalestier[2], Roberto Amato[6], Richard D. Pearson[6], Alexander B. Taylor[7], François H. Nosten[8], Umberto D'Alessandro[1], Dominic Kwiatkowski [6], Ian H. Cheeseman[9], Stefan H. I. Kappe[4,10,11], Simon V. Avery[5], David J. Conway[12], Ashley M. Vaughan[4,10†], Michael T. Ferdig[2†], Timothy J. C. Anderson[3†]

[1]MRC Unit The Gambia at London School of Hygiene and Tropical Medicine, Banjul, The Gambia

[2]Eck Institute for Global Health, Department of Biological Sciences, University of Notre Dame, Notre Dame, IN, USA

[3]Disease Intervention and Prevention Program, Texas Biomedical Research Institute, San Antonio, TX, USA

[4]Center for Global Infectious Disease Research, Seattle Children's Research Institute, Seattle, WA, USA

[5]School of Life Sciences, University of Nottingham, Nottingham, UK

[6]Wellcome Sanger Institute, Hinxton, UK

[7]Department of Biochemistry & Structural Biology, University of Texas Health Science Center at San Antonio, TX, USA

[8]Shoklo Malaria Research Unit, Mahidol-Oxford Tropical Medicine Research Unit, Mahidol University, Mae Sot, Thailand; Centre for Tropical Medicine and Global Health, Nuffield Department of Medicine Research building, University of Oxford Old Road campus, Oxford, UK

[9]Host Pathogen Interactions Program, Texas Biomedical Research Institute, San Antonio, TX, USA

[10]Department of Pediatrics, University of Washington, Seattle, WA, USA

[11]Department of Global Health, University of Washington, Seattle, WA, USA

[12]Department of Infection Biology, London School of Hygiene and Tropical Medicine, London, UK

*These authors made equal contributions

† Corresponding authors

Abstract (125 words):
The chloroquine (CQ) resistance transporter (*pfcrt*) is the main focus of CQ-resistance research in *Plasmodium falciparum*, with little emphasis on the role of other loci. Longitudinal genomic analyses of Gambian parasites revealed temporal signatures of selection on the amino acid transporter (*pfaat1)*-S258L variant which increased from 0-87% in frequency between 1984 and 2014 in parallel with *pfcrt1*-K76T. We conducted parasite genetic crosses identifying a chromosome 6 quantitative trait locus (QTL) containing *pfaat1* that interacts epistatically with *pfcrt* to determine CQ-resistance. Gene editing demonstrated that *pfaat1*-S258L potentiates CQ-resistance but at a cost of reduced fitness, while *pfaat1*-F313S, a common Southeast Asian polymorphism, reduces CQ-resistance while restoring fitness. Our combined experimental and population genomic analyses reveal hidden complexity in CQ-resistance evolution and a central role for *pfaat1*.

One-Sentence Summary: Utilizing historical *P. falciparum* population genomic data, parasite genetic crosses, and gene editing, we show that *pfaat1* interacts epistatically with *pfcrt* to modulate chloroquine resistance and parasite fitness.

Drug resistance in microbial pathogens complicates control efforts. Therefore, understanding the genetic architecture and the complexity of resistance evolution is critical for resistance monitoring and the development of improved treatment strategies. In the case of malaria parasites, deployment of five classes of antimalarial drugs over the last half century have resulted in well-characterized hard and soft selective sweeps, with both worldwide dissemination and local origins of resistance driving drug resistance alleles across the range of *P. falciparum (1-3)*. Chloroquine (CQ) monotherapy played a central role in an ambitious plan to eradicate malaria in the last century. Resistance to CQ was first observed in 1957 in Southeast Asia, and subsequently arrived and spread across Africa from the late 1970s, contributing to the end of global eradication efforts (*4*).

Resistance to CQ has been studied intensively. The chloroquine resistance transporter (*pfcrt*, chromosome [chr.] 7) was originally identified using a *P. falciparum* genetic cross conducted between a CQ-resistant Southeast Asian (SEA) parasite and a CQ-sensitive South American parasite generated in a chimpanzee host (*5, 6*). Twenty years of intensive research revealed the mechanistic role of CRT in drug resistance (*7, 8*), its location in the food vacuole membrane, and its natural function transporting short peptides from the food vacuole into the cytoplasm (*9*). CQ kills parasites by interfering with hemoglobin digestion in the parasite food vacuole, preventing conversion of heme, a toxic by-product of hemoglobin digestion, into inert hemozoin crystals. Parasites carrying CQ-resistance mutations at CRT transport CQ out of the food vacuole, away from the site of drug action (*7, 8*). The *pfcrt* K76T single nucleotide polymorphism (SNP) is widely used as a molecular marker for CQ resistance (*10*), while additional variants within *pfcrt* modulate levels of resistance to CQ (*11*) and other quinoline drugs (*12*), and determine associated fitness costs (*13*). While mutations in a second transporter located in the food vacuole membrane, the multidrug resistance transporter (*pfmdr1)*, have been shown to modulate CQ resistance in some genetic backgrounds (*14*), the role of other genes in chloroquine resistance evolution remains unclear. In this work we sought to understand the contribution of additional parasite loci to CQ-resistance evolution using a combination of population genomics, experimental genetic crosses, and gene editing.

Results

Strong signatures of selection on pfaat1

Longitudinal population genomic data can provide compelling evidence of the evolution of drug resistance loci (*15*). We conducted a longitudinal whole genome sequence analysis of 600 *P. falciparum* genomes collected between 1984 and 2014 in The Gambia to examine signatures of selection (Table S1) under drug pressure. Following filtration using genotype missingness (<10%) and minor allele frequency (>2%), we retained 16,385 biallelic SNP loci from 321 isolates (1984 [134], 1990 [13], 2001 [34], 2008 [75], and 2014 [65]. The *pfcrt* K76T allele associated with CQ-resistance increased from 0% in 1984 to 70% in 2014 and intriguingly, an S258L mutation in the amino acid transporter, *pfaat1* (PF3D7_0629500, chr. 6) increased during the same time period from 0% to 87% (Fig 1A). Assuming a generation time (mosquito to mosquito) of 6 months for malaria parasites, these changes were driven by selection coefficients of 0.18 for *pfaat1* S258L, and 0.12 for *pfcrt* K76T (Fig. S1). Both *pfaat1* and *pfcrt* showed similar temporal haplotype structures in The Gambia (Fig. S2). These were characterized by almost complete replacement of well differentiated haplotypes at both loci between 1984 and 2014. During this period, we also observed major temporal changes in another known drug resistance locus (*pfdhfr*) (chr. 4) (Fig. 1B) (*16*).

Further evidence of strong selection on *pfaat1* and *pfcrt* came from the analysis of identity-by-descent (IBD) in Gambian parasite genomes. We saw the strongest signals of IBD in the genome around both *pfaat1* and *pfcrt* (Fig. 1C). These signals are dramatic, because there is minimal IBD elsewhere in the genome, with the exception of a strong signal centering on *pfdhfr* after 2008. Interestingly, the strong IBD is observed in all four temporal samples examined including 1984, prior to the spread of either *pfaat1* S258L or *pfcrt* K76T. However, only a single synonymous variant coding for *pfaat1* (I552) and none of the CQ-resistant associated mutant variants in *pfcrt* were present at that time. These results are consistent with the possibility of CQ-driven selective sweeps prior to 1984, perhaps targeting promotor regions of these genes.

Patterns of linkage disequilibrium (LD) provide further evidence for functional linkage between *pfcrt* and *pfaat1*. The strongest genome-wide signal of interchromosomal LD was found between these two loci (Fig. S3) (*17*). LD between *pfaat1* and *pfcrt* was strongest in 2001, and then decayed in 2008 and 2014 (Fig. S3), consistent with maintenance of LD during intensive CQ usage, and subsequent LD decay after CQ monotherapy was replaced by sulfadoxine-pyrimethamine + CQ combinations in 2004, and then with artemisinin combinations in 2008 (*16*).

Divergent selection on pfaat1 in Southeast Asia

We examined the haplotype structure of *pfaat1* from *P. falciparum* genomes (MalariaGEN release 6 (*18*)) (Fig. 2A, Table S2). The *pfaat1* S258L SNP is at high frequency in SEA (58%) but is found on divergent flanking haplotypes consistent with an independent origin from the *pfaat1* S258L in The Gambia and elsewhere in Africa (Fig. 2B, Fig. S4-5, (*19*)). Convergent evolution of *pfaat1* S258L provides further evidence for selection, and contrasts with *pfcrt* and *pfdhfr*, where resistance alleles that spread in Africa had an Asian origin (*1, 2*). *Pfaat1* evolution is more complex in SEA than elsewhere in the world. There are three additional common derived amino acid changes in SEA. *pfaat1* F313S has spread close to fixation in SEA (total 96%, F_{ST} = 0.91 compared with African samples) paired with *pfaat1* S258L (55%), Q454E (15%), and K541N (22%). We speculate that these geographically localized *pfaat1* haplotypes have played an important role in CQ-resistance evolution in SEA and could also reflect geographic differences in the historical use of other quinoline drugs (mefloquine, quinine, piperaquine, lumefantrine) in this region (*20*).

Parasite genetic crosses using humanized mice identify a QTL containing pfaat1

P. falciparum genetic crosses can be achieved with human-liver chimeric mice, reviving and enhancing this powerful tool for malaria genetics (*21, 22*) after use of great apes for research was banned. We conducted three independent biological replicates of a cross between the CQ-sensitive West African parasite, 3D7, and a recently isolated CQ-resistant parasite from the Thailand-Myanmar border, NHP4026 (Table S3). We then compared genome-wide allele frequencies in CQ-treated and control-treated progeny pools to identify quantitative trait loci (QTL). This bulk segregant analysis (BSA) (*23*) of progeny parasites robustly identified the chr. 7 locus containing *pfcrt* as expected, validating our approach (Fig. 3A and Fig. S6-7). We were also intrigued to see a significant QTL on chr. 6 in each of the replicate crosses (Fig. 3, Fig. S8). We prioritized genes within the 95% confidence interval of each QTL (Table S4) by inspecting the SNPs and indels that differentiated the two parents (Table S5). The chr. 6 QTL spanned from 1,013 kb to 1,283kb (270 kb), and contained 60 genes. Of these, 54 are expressed in blood stages, and 27 have non-synonymous mutations that differentiate 3D7 from NHP4026. *pfaat1* was located at the peak of the chr. 6 QTL (Fig. 3C). NHP4026 carried two derived non-

synonymous mutations in *pfaat1* (S258L and F313S) compared to 3D7, which carries the ancestral allele at each of these codon sites. We thus hypothesized that one or both of these *pfaat1* SNPs may be driving the chr. 6 QTL.

BSA provides an efficient approach to identifying QTLs but cannot determine whether there are epistatic interactions between QTLs. To address this, we isolated individual clones from the bulk 3D7 × NHP4026 F_1 progeny to recover clones with all combinations of parental alleles at the chr. 6 and chr. 7 QTL loci. We cloned parasites both from a bulk progeny culture that was CQ-selected (96 hours at 250 nM CQ) and from a control culture. This generated 155 clonal progeny: 100 from the CQ-selected culture, 62 of which were genetically unique and 55 from the untreated control culture, of which 47 were unique (Fig. 4A). We compared allele frequencies between these two progeny populations (Fig. 4B), revealing significant differences at both chr. 6 and chr. 7 QTL regions, paralleling the BSA results. We observed a dramatic depletion of the NHP4026 CQ-resistant allele at the chr. 7 QTL in control treated cultures, consistent with strong selection against CQ resistant *pfcrt* alleles in the absence of CQ-selection. Conversely, all progeny isolated after CQ treatment harbored the NHP4026 CQ-resistant *pfcrt* allele. The inheritance of the *pfcrt* locus (chr. 7) and the *pfaat1* locus (chr. 6) was tightly linked in the isolated clones (Fig. 4C). These results are consistent with the strong LD between these loci observed in nature (Fig. S3) (*17*) and suggest co-selection of unlinked genes under CQ drug pressure and a functional relationship between the two loci.

We next measured *in vitro* CQ IC_{50} values for 18 parasites (a set of 16 progeny and both parents), carrying all combinations of the chr. 6 and chr. 7 QTL alleles (Fig. 4D, Table S6). The NHP4026 parent was the most CQ-resistant parasite tested. All progeny that inherited NHP4026 *pfcrt* showed a CQ-resistant phenotype while all progeny that inherited 3D7 *pfcrt* were CQ-sensitive, consistent with previous reports. The *pfcrt* effect was significant in a two-way ANOVA ($p=2.2 \times 10^{-16}$) accounting for 60% of the total variation in CQ IC_{50}, while the chr. 6 effect ($p=5.6 \times 10^{-13}$) explained a further 16% of the total variation in CQ IC_{50}. A significant epistatic interaction was observed between the two unlinked loci (p=0.003): chr. 6 contributed to elevated CQ IC_{50} only in progeny carrying the CQR *pfcrt* K76T allele inherited from NHP4026 (p=0.01) but not in progeny that inherited *pfcrt* from 3D7 (p=0.55). These results demonstrate that the chr. 6 QTL interacts epistatically with *pfcrt* to elevate CQ-resistance.

Functional validation of the role of pfaat1 in CQ resistance

We next utilized CRISPR/Cas9 modification of the NHP4026 CQ-resistant parent to investigate the effects of mutations in *pfaat1* on CQ IC_{50} drug response and parasite fitness (Fig. 5). NHP4026 *pfaat1* contains two derived non-synonymous changes (S258L and F313S), common in SEA (Fig. 2), relative to the sensitive 3D7 parent. We edited these positions back to the ancestral state both singly and in combination and confirmed the modifications in three clones isolated from independent CRISPR experiments for each allelic change. We then determined CQ IC_{50} and measured fitness using pairwise competition experiments for $NHP4026^{258\underline{L}/313\underline{S}}$, $NHP4026^{258\underline{L}/313F}$, $NHP4026^{258S/313\underline{S}}$ and $NHP4026^{258S/313F}$. This revealed a highly significant impact of the S258L mutation, which increases CQ IC_{50} 1.5-fold, and a more moderate but significant impact of F313S and the double mutation (S258L/F313S) (Fig. 5B, Table S7). The small differences in IC_{50} between *pfaat1*-wild-type (WT) and the double mutation (S258L/F313S) are also consistent with the moderate, but significant chr. 6 QTL seen in our genetic cross. The observation that 258L shows an elevated IC_{50} only in combination with the ancestral 313F allele reveals epistatic interactions between these amino acid variants (Fig 5B) within AAT1.

Mutations conferring drug resistance may carry fitness costs in the absence of drug treatment. We examined parasite fitness in culture by conducting pairwise competition experiments against a common competitor (NHP4026$^{258L/313S}$), which revealed significant differences in fitness of the parasites carrying different alleles at *pfaat1* (Fig. 5C). The 258L/313F allele that showed a selective sweep in The Gambia, was the least fit of all genotypes. The ancestral allele (258S/313F) carried by the 3D7 parent showed the highest fitness, while the 258L/313S double mutation, that predominates in western SEA, and the 258S/313S show intermediate fitness. The differences in fitness observed between the alleles were extremely strong: for example, the difference in fitness between *pfaat1*-WT and *pfaat1*-S258L is 0.31 per 48 h asexual cycle (Fig. 5C). We also saw strong epistatic interactions in fitness (Fig 5C). While the 258L/313F allele conferring high CQ IC_{50} carried a heavy fitness penalty, fitness was partially restored by addition of the F313S mutation to generate the 258L/313S allele that predominates in SEA. Together these results show that the *pfaat1* S258L substitution underpins a 1.5-fold increase in CQ-resistance that likely drove its selective spread in The Gambia. However, S258L carries a high fitness cost that is mitigated by addition of a compensatory substitution, F313S, as observed in SEA parasites.

To further understand how *pfaat1* S258L impacts parasite phenotype, we used a yeast heterologous expression system. WT *pfaat1* expression in the yeast plasma membrane increases quinine and CQ uptake conferring drug sensitivity to quinoline drugs, but is competitively inhibited by the aromatic amino acid tryptophan, suggesting a role for *pfaat1* in drug transport (*24*). We therefore expressed *pfaat1*-258L in yeast, which restored yeast growth in the presence of high levels of CQ (Fig. S9). Interestingly, expression of another variant amino acid (T162E), responsible for CQ-resistance in rodent malaria parasites (*P. chabaudi*) (*25*), also prevents accumulation of quinoline drugs within yeast cells (*24*). Together, these results suggest that mutations in *pfaat1* in yeast may impact resistance and fitness by altering the rate of amino acid or CQ transport.

To investigate the relationship between AAT1 mutations, protein structure, and function, we evaluated three-dimensional structural models based on the 3D7 AAT1 amino acid sequence using AlphaFold (*26*) and I-TASSER (*27*) (Fig. S10). While CRT has ten membrane-spanning helices (*8*), AAT1 has eleven; this was corroborated using the sequence-based membrane topology prediction tool TOPCONS (*28*). AAT1 S258L, F313S and Q454E are situated in the membrane-spanning regions, while K541L is in a loop linking helices 9 and 10. The substitution of serine with the bulkier, hydrophobic leucine at position 258 could alter interactions with its neighboring transmembrane helices including helix 8. Residue 313 maps to helix 5 on the other side of helix 8, opposite to residue 258. Given the epistatic interactions between the AAT1 S258L and F313S SNPs evident from the functional analysis, the F313S substitution of the bulky, hydrophobic phenylalanine with the smaller, polar serine may compensate for a disruption in the transmembrane region that includes helices 3, 5, and 8 allowing for partial restoration of activity.

Discussion

Identification of *pfcrt* as the major determinant of CQ resistance was a breakthrough that transformed the malaria drug resistance research landscape, but the contribution of additional genetic factors in the evolution and maintenance of CQ resistance remained unclear (*29, 30*). By combining longitudinal population genomic analysis spanning the emergence of CQ resistance in

The Gambia, analysis of bulk populations and progeny from controlled genetic crosses, phenotyping of cloned progeny, and functional validation using both yeast and *P. falciparum*, we find clear evidence that a second locus, *pfaat1*, has played a central role in CQ resistance. This powerful combination of approaches allowed us to examine critical *pfaat1* variants that contribute to the architecture of CQ-resistance and interactions between *pfcrt and pfaat1*.

Our results provide compelling evidence that consolidates disparate observations from several systems suggesting a role for *pfaat1* in drug resistance evolution. In the rodent malaria parasite *P. chabaudi*, a mutation (T162E) in the orthologous amino acid transporter (*pcaat1*) was found to be a determinant of low level CQ resistance in laboratory-evolved resistance (*25*). In *P. falciparum* genome-wide association studies (GWAS), the S258L mutation of *pfaat1* was associated with CQ resistance in field isolates collected along the China-Myanmar border (*31*), while *pfcrt*-K76T and *pfaat1*-S258L show the strongest LD between physically unlinked chromosomes genome-wide (*17*). In addition, mutations in *pfaat1* have been linked to the *in vitro* evolution of resistance in *P. falciparum* to three different drug scaffolds (*32*). Previous work identified strong signatures of recent selection in parasites in Africa at regions surrounding *pfcrt*, *pfaat1*, and other drug resistance loci (*16, 33, 34*); similar signatures of selection are seen in Asia and South America (*19, 35*) while *pfaat1* was highlighted in a list of *P. falciparum* genes showing extreme geographical differentiation (*18*).

The different *pfaat1* haplotypes in Africa and Asia may be partly responsible for the contrasting evolution of CQ-resistance in these two continents. CQ-resistant parasites, carrying both *pfcrt* K76T and *pfaat1* S258L spread across Africa, but after removal of CQ as the first line drug, the prevalence of CQ resistant parasites declined in many countries (*36-38*). This is consistent with the low fitness of parasites carrying *pfcrt* K76T and *pfaat1* S258L in the absence of drug pressure. In contrast, *pfcrt* K76T has remained at or near fixation in many SEA countries (*18, 39*) (Fig. 2), and on the Thailand-Myanmar border, CQ-resistance has remained at fixation since 1995, when CQ was removed as first line treatment of *P. falciparum* malaria (*39*). Our *pfaat1* mutagenesis results demonstrate that parasites bearing *pfaat1* 258L/313S show reduced IC_{50}, but elevated fitness relative to *pfaat1* 258L/313F. Together with continued use of CQ to treat *P. vivax (40)*, the restoration of fitness by F313S may help to explain retention of CQ-resistant *pfcrt* K76T alleles in SEA. It is also possible that different *pfaat1* allele frequencies have resulted from the geographically divergent histories of treatment with other antimalarial drugs (*41*).

Mutations in *pfcrt* confer CQ-resistance by enabling efflux of CQ from the digestive vacuole and away from their site of action (*8*). AAT1 is also located in the food vacuole membrane, where it likely acts as a bidirectional transporter of aromatic amino acids (*9, 42*). Given the structural similarity of quinoline drugs and aromatic amino acids, *pfaat1* mutations may modulate the ability of AAT1 to transport CQ and/or amino acids (*24, 42*). The *pfaat1* S258L mutation could potentiate resistance by either increasing efflux of CQ out of the digestive vacuole or reducing the rate of entry into the vacuole. Given that this *pfaat1* mutation blocks entry of quinoline drugs into yeast cells when heterologously expressed in the yeast cell membrane (*24*), we hypothesize that the *pfaat1* S258L mutation reduces CQ uptake into the food vacuole (Fig. 6). Our mutagenesis analyses show that the S258L allele has a high fitness cost, perhaps due to a decreased capacity for the amino acid transport from the vacuole. Interestingly, comparison of the *pfaat1* S258L/F313S haplotype segregating in our genetic cross with the WT *pfaat1* allele generated using gene editing, revealed only marginal increases in IC_{50} and limited reductions in fitness. This is consistent with the F313S mutation restoring the natural *pfaat1* function of transporting amino acids, thereby reducing osmotic stress and starvation, while also partially

reducing levels of CQ-resistance. That this haplotype has reached high frequency in SE Asia, may contribute to the maintenance of *pfcrt* K76T alleles long after the removal of CQ as a first line drug.

Our results reveal hidden complexity in CQ-resistance evolution: drug treatment has driven global selective sweeps acting on mutations in an additional transporter (AAT1) located in the *P. falciparum* food vacuole membrane, which fine tune the balance between nutrient and drug transport, revealing evidence for epistasis and compensation, and impacting both drug resistance and fitness.

References and Notes

1. J. C. Wootton *et al.*, Genetic diversity and chloroquine selective sweeps in Plasmodium falciparum. *Nature* **418**, 320-323 (2002).
2. C. Roper *et al.*, Intercontinental spread of pyrimethamine-resistant malaria. *Science (New York, N.Y.)* **305**, 1124 (2004).
3. F. Ariey *et al.*, A molecular marker of artemisinin-resistant *Plasmodium falciparum* malaria. *Nature* **505**, 50-55 (2014).
4. T. E. Wellems, C. V. Plowe, Chloroquine-resistant malaria. *The Journal of infectious diseases* **184**, 770-776 (2001).
5. X. Su, L. A. Kirkman, H. Fujioka, T. E. Wellems, complex polymorphisms in an ~330 kDa protein are linked to chloroquine-resistant P. falciparum in southeast Asia and Africa. *Cell* **91**, 593-603 (1997).
6. T. E. Wellems, A. Walker-Jonah, L. J. Panton, Genetic mapping of the chloroquine-resistance locus on *Plasmodium falciparum* chromosome 7. *Proc Natl Acad Sci U S A* **88**, 3382-3386 (1991).
7. D. A. Fidock *et al.*, Mutations in the P. falciparum digestive vacuole transmembrane protein PfCRT and evidence for their role in chloroquine resistance. *Molecular Cell* **6**, 861-871 (2000).
8. A. Ecker, A. M. Lehane, J. Clain, D. A. Fidock, PfCRT and its role in antimalarial drug resistance. *Trends in Parasitology* **28**, 504-514 (2012).
9. S. H. Shafik *et al.*, The natural function of the malaria parasite's chloroquine resistance transporter. *Nature communications* **11**, 3922 (2020).
10. A. Djimde *et al.*, A molecular marker for chloroquine-resistant falciparum malaria. *N Engl J Med* **344**, 257-263 (2001).
11. S. Pelleau *et al.*, Adaptive evolution of malaria parasites in French Guiana: Reversal of chloroquine resistance by acquisition of a mutation in pfcrt. *Proceedings of the National Academy of Sciences of the United States of America* **112**, 11672-11677 (2015).
12. L. S. Ross *et al.*, Emerging Southeast Asian PfCRT mutations confer *Plasmodium falciparum* resistance to the first-line antimalarial piperaquine. *Nature communications* **9**, 3314 (2018).
13. S. K. Dhingra *et al.*, Global Spread of Mutant PfCRT and Its Pleiotropic Impact on *Plasmodium falciparum* Multidrug Resistance and Fitness. *mBio* **10**, (2019).
14. S. H. Shafik, S. N. Richards, B. Corry, R. E. Martin, Mechanistic basis for multidrug resistance and collateral drug sensitivity conferred to the malaria parasite by polymorphisms in PfMDR1 and PfCRT. *PLoS biology* **20**, e3001616 (2022).

15. G. C. Cerqueira *et al.*, Longitudinal genomic surveillance of *Plasmodium falciparum* malaria parasites reveals complex genomic architecture of emerging artemisinin resistance. *Genome biology* **18**, 78 (2017).
16. D. C. Nwakanma *et al.*, Changes in malaria parasite drug resistance in an endemic population over a 25-year period with resulting genomic evidence of selection. *The Journal of infectious diseases* **209**, 1126-1135 (2014).
17. G. Band *et al.*, Malaria protection due to sickle haemoglobin depends on parasite genotype. *Nature* **602**, 106-111 (2022).
18. MalariaGEN *et al.*, An open dataset of *Plasmodium falciparum* genome variation in 7,000 worldwide samples. *Wellcome open research* **6**, 42 (2021).
19. L. Henden, S. Lee, I. Mueller, A. Barry, M. Bahlo, Identity-by-descent analyses for measuring population dynamics and selection in recombining pathogens. *PLoS genetics* **14**, e1007279 (2018).
20. R. E. Martin, S. H. Shafik, S. N. Richards, Mechanisms of resistance to the partner drugs of artemisinin in the malaria parasite. *Current opinion in pharmacology* **42**, 71-80 (2018).
21. K. M. Vendrely, S. Kumar, X. Li, A. M. Vaughan, Humanized Mice and the Rebirth of Malaria Genetic Crosses. *Trends in Parasitology*, (2020).
22. A. M. Vaughan *et al.*, *Plasmodium falciparum* genetic crosses in a humanized mouse model. *Nature Methods* **12**, 631-633 (2015).
23. K. V. Brenneman *et al.*, Optimizing bulk segregant analysis of drug resistance using *Plasmodium falciparum* genetic crosses conducted in humanized mice. *iScience* **25**, 104095 (2022).
24. S. M. Tindall *et al.*, Heterologous expression of a novel drug transporter from the malaria parasite alters resistance to quinoline antimalarials. *Scientific Reports* **8**, (2018).
25. K. K. Modrzynska *et al.*, Quantitative genome re-sequencing defines multiple mutations conferring chloroquine resistance in rodent malaria. *BMC Genomics* **13**, (2012).
26. J. Jumper *et al.*, Highly accurate protein structure prediction with AlphaFold. *Nature* **596**, 583-589 (2021).
27. J. Yang *et al.*, The I-TASSER Suite: protein structure and function prediction. *Nature methods* **12**, 7-8 (2015).
28. K. D. Tsirigos, C. Peters, N. Shu, L. Käll, A. Elofsson, The TOPCONS web server for consensus prediction of membrane protein topology and signal peptides. *Nucleic acids research* **43**, W401-407 (2015).
29. P. S. Callaghan, M. R. Hassett, P. D. Roepe, Functional comparison of 45 naturally occurring isoforms of the *Plasmodium falciparum* chloroquine resistance transporter (PfCRT). *Biochemistry* **54**, 5083-5094 (2015).
30. J. J. Patel *et al.*, Chloroquine susceptibility and reversibility in a *Plasmodium falciparum* genetic cross. *Molecular microbiology* **78**, 770-787 (2010).
31. Z. Wang *et al.*, Genome-wide association analysis identifies genetic loci associated with resistance to multiple antimalarials in *Plasmodium falciparum* from China-Myanmar border. *Scientific Reports* **6**, (2016).
32. A. N. Cowell *et al.*, Mapping the malaria parasite druggable genome by using in vitro evolution and chemogenomics. *Science (New York, N.Y.)* **359**, 191-199 (2018).
33. A. Amambua-Ngwa *et al.*, Major subpopulations of *Plasmodium falciparum* in sub-Saharan Africa. *Science* **365**, 813-816 (2019).
34. A. Amambua-Ngwa *et al.*, SNP genotyping identifies new signatures of selection in a deep sample of West African *Plasmodium falciparum* malaria parasites. *Molecular biology and evolution* **29**, 3249-3253 (2012).

35. M. Carrasquilla *et al.*, Resolving drug selection and migration in an inbred South American *Plasmodium falciparum* population with identity-by-descent analysis. *bioRxiv : the preprint server for biology*, 2022.2002.2018.480973 (2022).
36. M. K. Laufer *et al.*, Return of chloroquine-susceptible falciparum malaria in Malawi was a reexpansion of diverse susceptible parasites. *J Infect Dis* **202**, 801-808 (2010).
37. J. G. Kublin *et al.*, Reemergence of chloroquine-sensitive *Plasmodium falciparum* malaria after cessation of chloroquine use in Malawi. *The Journal of infectious diseases* **187**, 1870-1875 (2003).
38. S. Mharakurwa *et al.*, Steep rebound of chloroquine-sensitive *Plasmodium falciparum* in Zimbabwe. *The Journal of infectious diseases* **223**, 306-309 (2021).
39. T. J. Anderson *et al.*, Geographical distribution of selected and putatively neutral SNPs in Southeast Asian malaria parasites. *Molecular biology and evolution* **22**, 2362-2374 (2005).
40. C. S. Chu *et al.*, Comparison of the cumulative efficacy and eafety of chloroquine, artesunate, and chloroquine-primaquine in Plasmodium vivax malaria. *Clinical infectious diseases : an official publication of the Infectious Diseases Society of America* **67**, 1543-1549 (2018).
41. E. A. Ashley, A. P. Phyo, Drugs in Development for Malaria. *Drugs* **78**, 861-879 (2018).
42. R. E. Martin, The transportome of the malaria parasite. *Biological reviews of the Cambridge Philosophical Society* **95**, 305-332 (2020).

Acknowledgments:

We thank past and present staff and visiting researchers at the MRC Unit in The Gambia involved in studies from which samples were archived, including those under the earlier directorships of Prof Brian Greenwood and Prof Tumani Corrah. Work at Texas Biomedical Research Institute was conducted in facilities constructed with support from Research Facilities Improvement Program grant C06 RR013556. SMRU is part of the Mahidol Oxford University Research Unit supported by the Wellcome Trust of Great Britain. We thank the staff of the Wellcome Trust Sanger Institute Sample Logistics, Sequencing and Informatics facilities for their contributions. The Structural Biology Core at The University of Texas Health Science Center at San Antonio is a part of Institutional Research Cores supported by the Office of the Vice President for Research and the Mays Cancer Center Drug Discovery and Structural Biology Shared Resource (National Institutes of Health grant P30 CA054174).

Funding:

National Institutes of Health grant P01 12072248 (MTF)

National Institutes of Health grant R37 AI048071 (TA)

MRC Career Development Fellowship MC_EX_MR/K02440X/1 (AAN)

MRC malaria program grant MC_EX_MR/J002364/1 (UDA)

European Research Council grant AdG-2011-294428 (DC and AAN)

MRC grant MR/S009760/1 (DC)

Wellcome Trust (206194, 204911) and the Bill & Melinda Gates Foundation (OPP1204628, INV-001927) (DK)

Biotechnology and Biological Sciences Research Council grant BB/M022161/1 (SVA)

Wellcome Trust [Grant number 220221] (FN); For the purpose of open access, the author has applied a CC BY public copyright license to any Author Accepted Manuscript version arising from this submission.

Author contributions:

Conceptualization: MTF, TA, IC, AV, AAN, DC

Methodology: AV, SK, SVA, ABT

Investigation: AAN, UDA, DK, DC, RA, RDP, KBS, KVB, LC, HD, JKL, AR, ED, SK, DS, ST, MF, ABT, TA

Analysis: XL, KBS, AAN

Visualization: XL, KBS, AAN

Funding acquisition : MTF, TA, DC, AAN, DK, SVA, FN

Project administration: MF, DK, AAN, DC, SVA

Supervision: MF, AV, TA, IC, SHIK, SVA, DK, DC

Writing – original draft: KVB, TA, KBS, XL

Writing – review & editing: MTF, AV, IC, SK, AAN, DC, DK, UDA, RDP, SHIK, FN, ABT, TA

Competing interests: Authors declare that they have no competing interests.

Data and materials availability: All data are available in the main text or the supplementary materials.

Supplementary Materials

Materials and Methods

Figs. S1 to S12

Tables S1 to S7

References (*1–30*)

Figure legends

Fig. 1. Rapid allele frequency change and strong signals of selection around *pfaat1* in The Gambia. (A) Temporal allele frequency change at SNPs coding for *pfaat1* S258L and the *pfcrt* K76T between 1984 and 2014. The map and expanded West African region show the location of The Gambia (B) Significance of haplotype differentiation across temporal populations of *P. falciparum* parasites determined using hapFLK. Regions within the top 1% tail of FDR-corrected *p*-values are marked with gene symbols. The strongest signals genome-wide seen are around *pfcrt*, *pfaat1*, and *pfdhfr* (the last of which is involved in pyrimethamine resistance). (C) Identity-by-descent (IBD), quantified with the isoRelate (iR) statistic, for temporal populations sampled

from The Gambia. Consistently high peaks of IBD around *pfcrt* and *pfaat1* are seen for parasite populations in all years of sampling.

Fig. 2. Distinctive trajectory of *pfaat1* evolution in Southeast Asia. (A) Global distribution of *pfaat1* alleles. We used dataset from MalariaGEN release 6 for *pfaat1* allele frequency analysis. Only samples with monoclonal infections (N = 4051) were included (1233 from West Africa, 415 from East Africa, 170 from Central Africa, 994 from east Southeast Asia, 998 from west Southeast Asia, 37 from South Asia, 37 from South America, and 167 from the Pacific Ocean region). Pie charts show allele distribution of *pfaat1*, and percentages next to the pie chart indicate *pfcrt* K76T frequency. (B) Minimum spanning networks of haplotypes from 50 kb genome regions centered around *pfaat1* (25 kb up- and down-stream). For clarity, only 581 genomes with the highest sequence coverage were used to generate the network. The networks were generated based on 1847 SNPs (at least one mutant in the full dataset - MalariaGEN release 6). Circle size indicates number of samples represented (smallest, 1; largest, 87). Haplotypes from the same region (Asia or Africa) were clustered together (see Fig. S5 for details), indicating independent origin of *pfaat1* alleles. (C) Color coding for the different *pfaat1* alleles.

Fig. 3. Genetic crosses and bulk segregant analysis reveal two QTL after CQ selection. (A) Allele frequency plots across the genome before and after CQ treatment. Lines with the same color indicate results from technical replicates. (B) QTLs identified using G' approach. Lines with the same color indicate results from technical replicates. (C) Fine mapping of the chr. 6 QTL. The 95% confidence intervals (CIs) were calculated from the 250 nM CQ treated samples (see Fig. S1 and S2), including data from different collection time points (day 4 for 48h CQ treatment and day 5 for 96h CQ treatment), pools (pool 1 and pool 2), and drug treatment duration (48 h and 96 h). Light cyan shadow shows boundaries of the merged CIs of all the QTLs. Each line indicates one QTL; black dashed line indicates threshold for QTL detection (G' = 20).

Fig. 4. Analysis of cloned progeny reveals linkage and epistatic interactions between *pfcrt* and *pfaat1*. (A) Allelic inheritance of 109 unique recombinant progeny. Vertical grey lines show non-core regions where no SNPs were genotyped (B) Allele frequency of the 3D7 allele in unique progeny cloned after 250 nM CQ selection for 96 hours (blue) and control (gold). (C) Linkage between loci on different chromosomes measured by Fisher's exact test. Dotted vertical line marks the Bonferroni corrected significance threshold, while points shown in red are comparisons between SNPs flanking in *pfaat1* and *pfcrt*. (D) Mean IC_{50} (+/- SD) of parents and selected progeny grouped by combinations of *pfcrt* and *pfaat1* allele.

Fig. 5. Allelic replacement impacts drug response and parasite fitness. (A) CRISPR/Cas9 gene editing. Starting with the NHP4026 parent, we generated all combinations of the SNP-states at *pfaat1*. (B) Drug response. Each dot indicates one replicate IC_{50} measurement: we used three independent CRISPR edited clones for each haplotype examined. Haplotypes are shown on the x-axis with derived amino acids shown in red. Bars show means, while significant differences between haplotypes are marked. (C) Fitness. The bars show relative fitness measured in replicated competition experiments conducted in the absence of CQ.

Fig. 6. Model for involvement of *pfaat1* haplotypes in CQ resistance and fitness. CRT (red) and AAT1 (blue) are both situated in the digestive vacuole (DV) membrane. (A) Wild-type CRT and AAT1 transport peptides and aromatic amino acids respectively. (B) CRT-76T exports CQ from the DV away from the cite of action of CQ, but transports peptides inefficiently leading to starvation and fitness loss (C) AAT1-S258L blocks entry of CQ into DV, leading to elevated

resistance, but increases starvation and osmotic stress. (D) AAT1-S258L/F313S reduces CQ blocking and/or restores amino acid transport function, leading to reduced IC_{50} and increased fitness in the absence of drug treatment.

Figure 1

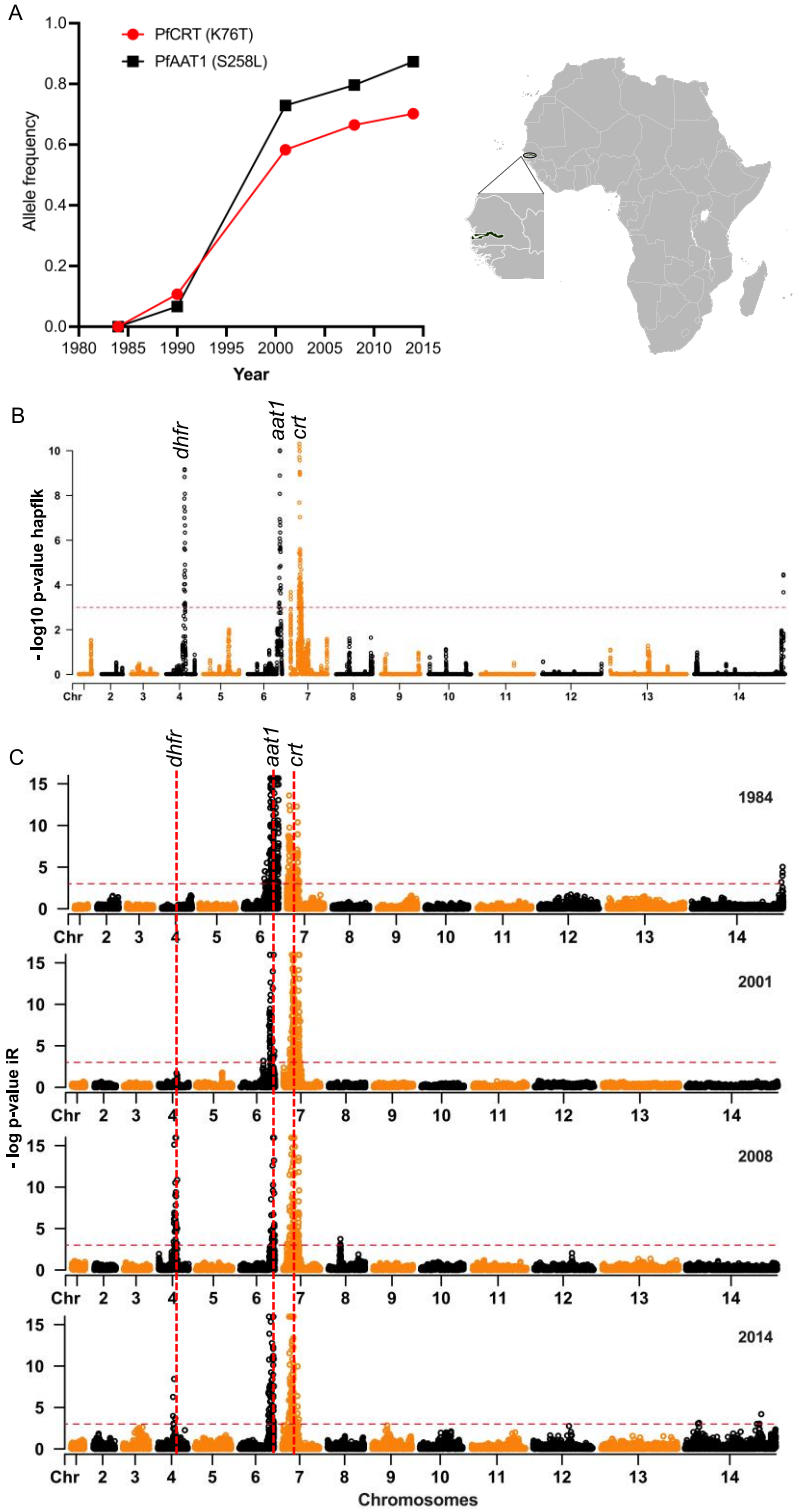
A
PfCRT (K76T)
PfAAT1 (S258L)
Allele frequency
Year
B
dhfr
aat1
crt
- log10 p-value hapflk
Chr
C
dhfr
aat1
crt
1984
2001
2008
2014
- log p-value iR
Chr
Chromosomes

Figure 2

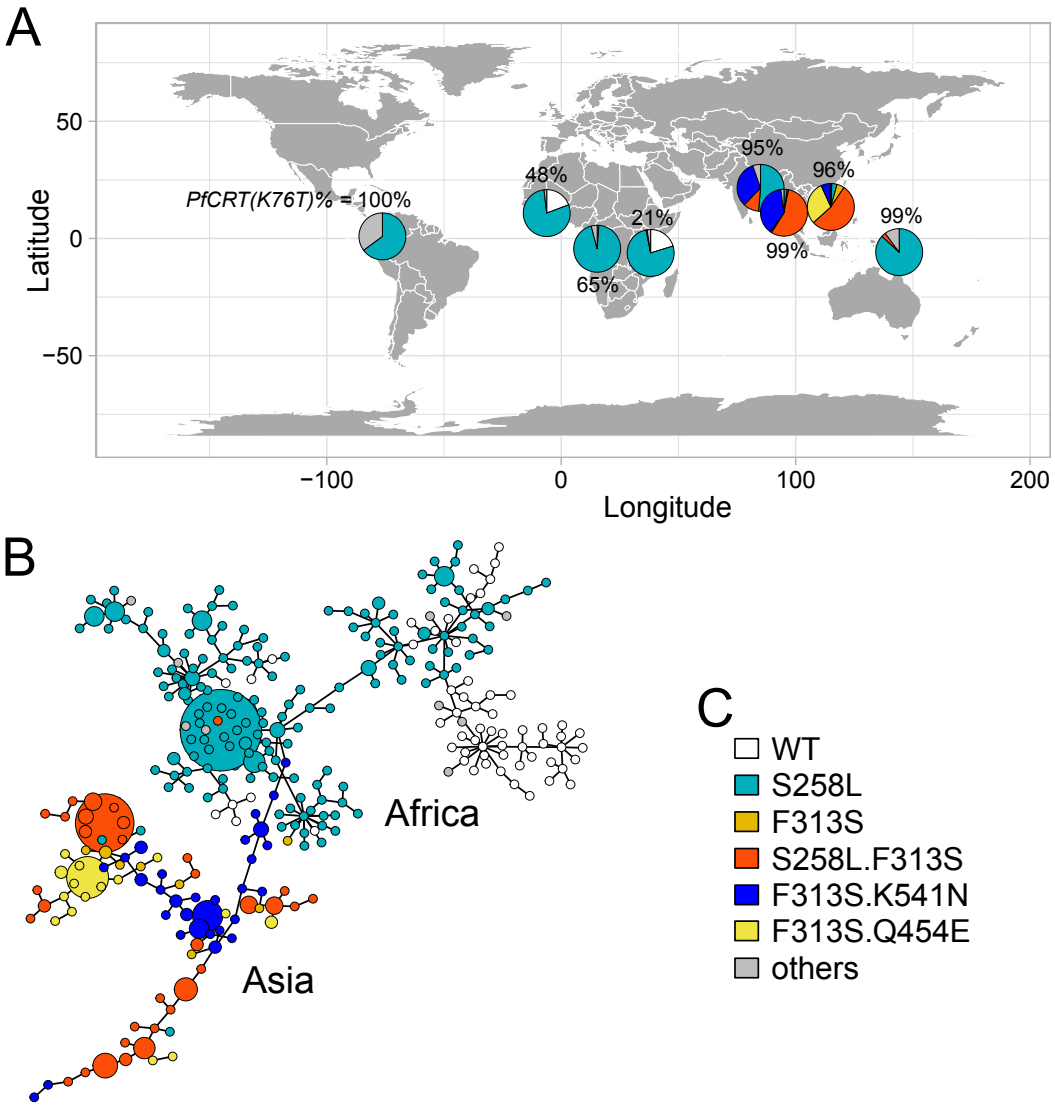
A
PfCRT(K76T)% = 100%
48%
65%
21%
95%
96%
99%
99%
Latitude
Longitude
50
0
−50
−100
0
100
200
B
Africa
Asia
C
WT
S258L
F313S
S258L.F313S
F313S.K541N
F313S.Q454E
others

Figure 3

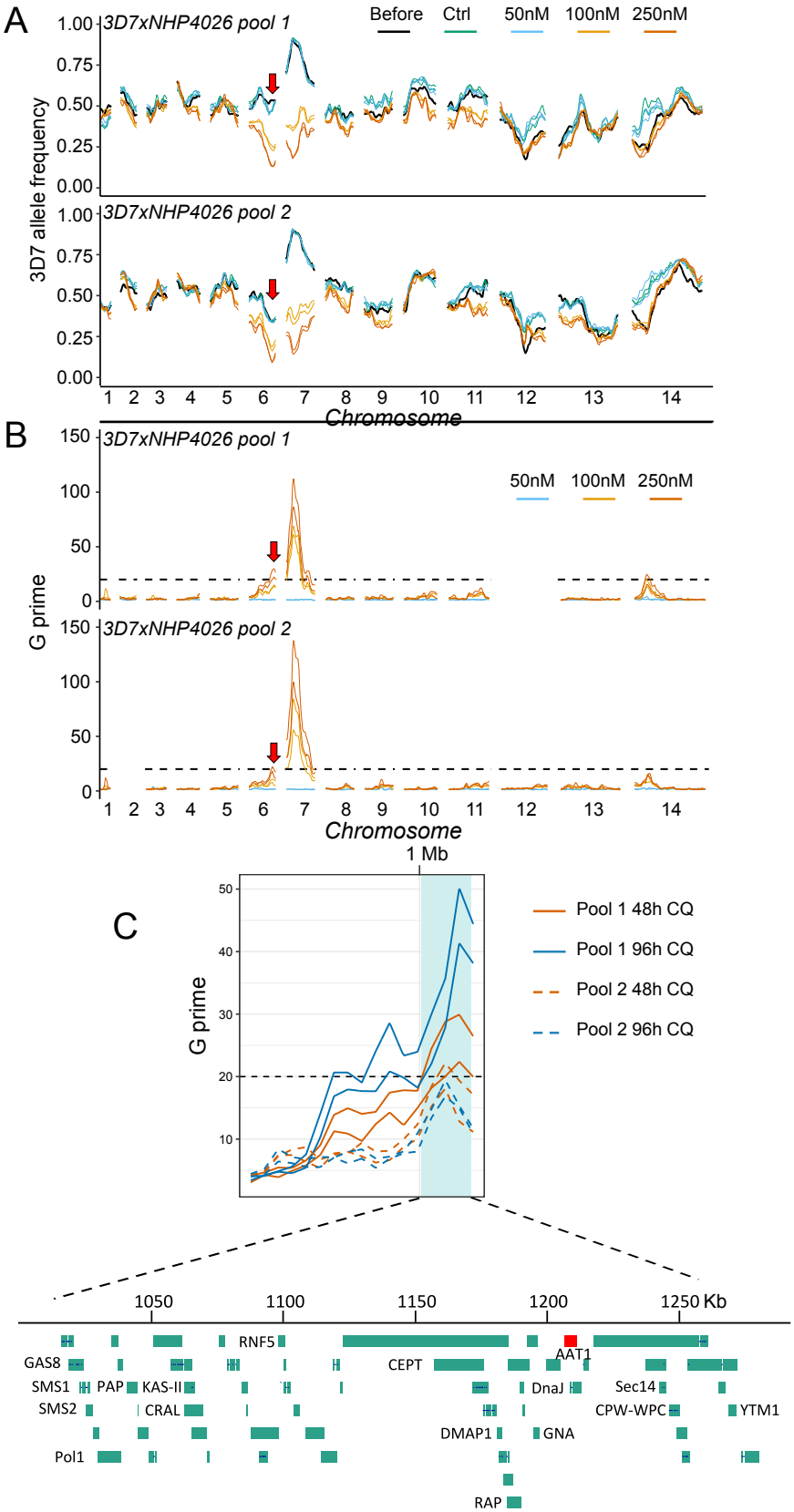
A
3D7xNHP4026 pool 1
Before
Ctrl
50nM
100nM
250nM
3D7 allele frequency
1.00
0.75
0.50
0.25
0.00
3D7xNHP4026 pool 2
1 2 3 4 5 6 7 8 9 10 11 12 13 14
Chromosome
B
3D7xNHP4026 pool 1
50nM
100nM
250nM
G prime
150
100
50
0
3D7xNHP4026 pool 2
1 2 3 4 5 6 7 8 9 10 11 12 13 14
Chromosome
C
1 Mb
G prime
50
40
30
20
10
Pool 1 48h CQ
Pool 1 96h CQ
Pool 2 48h CQ
Pool 2 96h CQ
1050
1100
1150
1200
1250 Kb
RNF5
AAT1
GAS8
CEPT
SMS1
PAP
KAS-II
DnaJ
Sec14
SMS2
CRAL
CPW-WPC
YTM1
DMAP1
GNA
Pol1
RAP

Figure 4

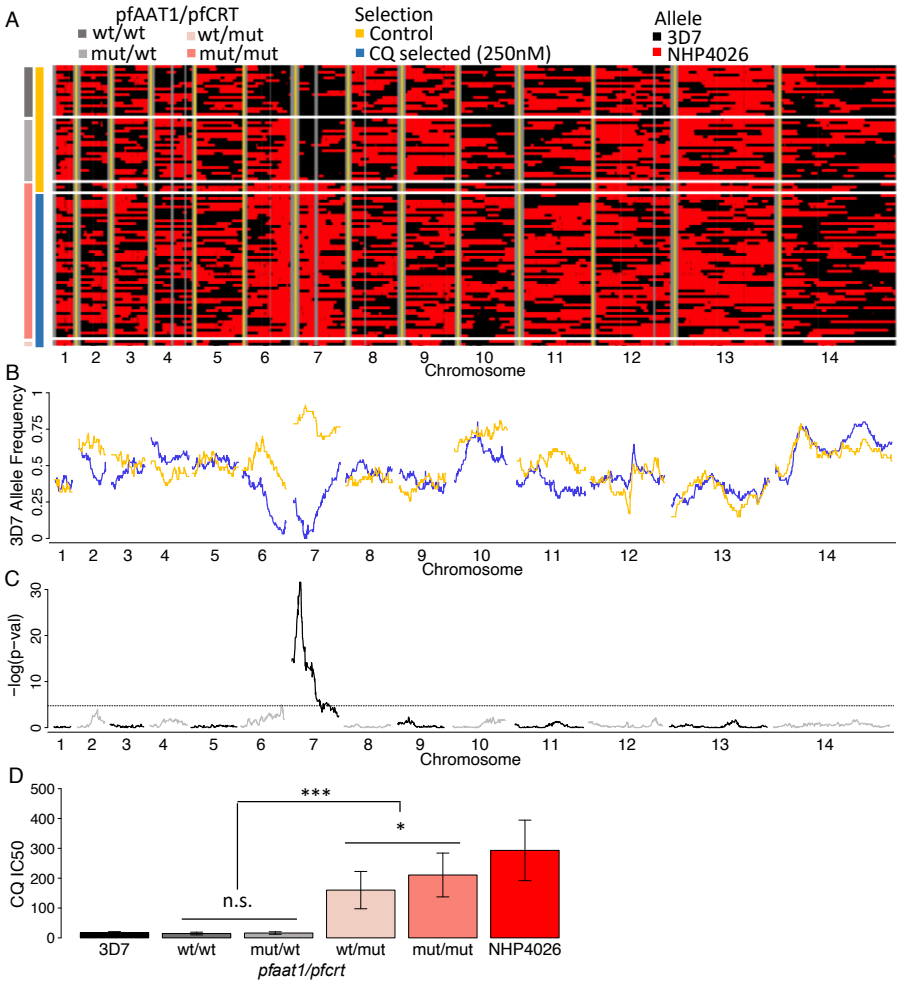
A
pfAAT1/pfCRT
wt/wt
wt/mut
mut/wt
mut/mut
Selection
Control
CQ selected (250nM)
Allele
3D7
NHP4026
1 2 3 4 5 6 7 8 9 10 11 12 13 14
Chromosome
B
3D7 Allele Frequency
0 0.25 0.5 0.75 1
1 2 3 4 5 6 7 8 9 10 11 12 13 14
Chromosome
C
−log(p−val)
0 10 20 30
1 2 3 4 5 6 7 8 9 10 11 12 13 14
Chromosome
D
CQ IC50
0 100 200 300 400 500
***
*
n.s.
3D7
wt/wt
mut/wt
wt/mut
mut/mut
NHP4026
pfaat1/pfcrt

Figure 5

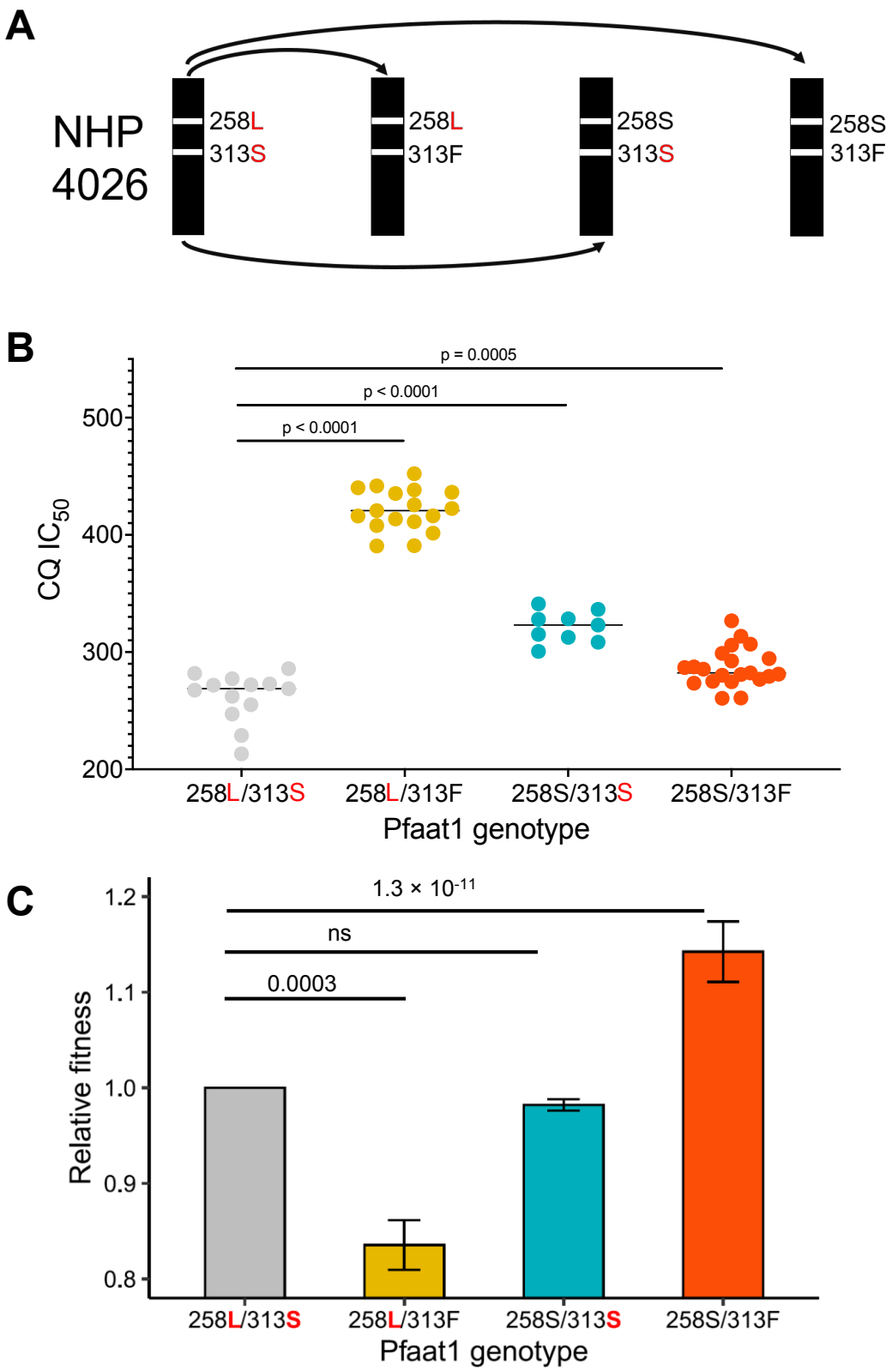
A
NHP 4026
258L
313S
258L
313F
258S
313S
258S
313F
B
p = 0.0005
p < 0.0001
p < 0.0001
CQ IC50
500
400
300
200
258L/313S
258L/313F
258S/313S
258S/313F
Pfaat1 genotype
C
1.3 × 10-11
ns
0.0003
Relative fitness
1.2
1.1
1.0
0.9
0.8
258L/313S
258L/313F
258S/313S
258S/313F
Pfaat1 genotype

Figure 6

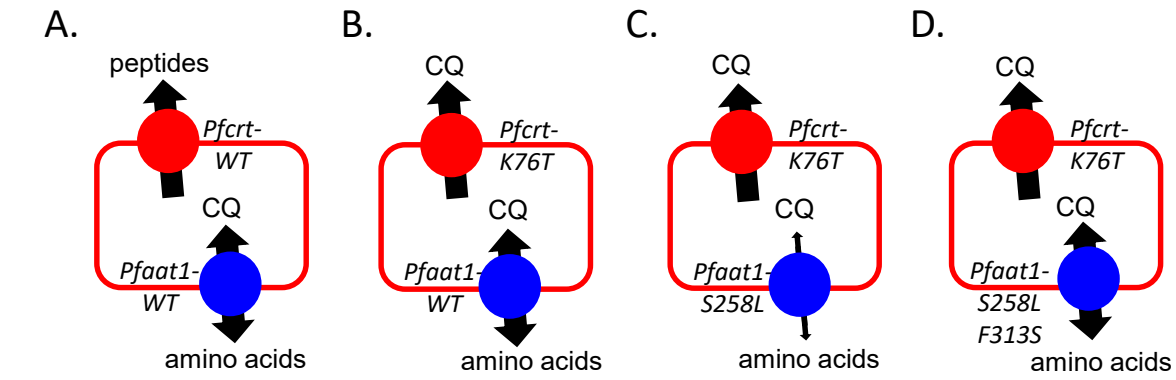

	A.	B.	C.	D.
Resistance	- - -	++	+++	++
Fitness	+++	++	+	++